

Encoding Accelerometer Signals as Images for Activity Recognition Using Residual Neural Network

Lu Jianjie¹, Tong Raymond²

¹ Department of Electronic Engineering jacklu@link.cuhk.edu.hk

² Department of Biomedical Engineering kytong@cuhk.edu.hk

The Chinese University of Hong Kong, Shatin, NT, Hong Kong SAR, China

Abstract

Human activity recognition using a single 3-axis accelerometer plays an important and fundamental role in daily monitoring using wearable sensors and devices. In this paper, we address the recognition problem by encoding 3-channel accelerometer signals as images and using transferring learning approach. Though projecting time series onto image space is not a new topic, our method is the first time to encode 3-axis signals as 3-channels of color images using recurrence plots (RP) and train an 18-layer Residual Neural Network (ResNet-18) to do image classification, to the best of our knowledge. We also first propose a modified RP to overcome its tendency confusion problem, which has improved our system performance significantly. A user-independent database of over 1080 traces with 5 actions from 11 subjects is used to test our method. In addition, we evaluate its generalization ability on a public dataset. Experimental results have shown that our recognition framework achieves highly competitive accuracies with other state-of-the-art methods on both datasets. And it has a great potential to be applied for 3-axis accelerometer signals recognition.

Introduction

Daily monitoring and home healthcare are becoming increasingly popular due to the proliferation of personal electronic devices like smartphone and wearable whist band. Accurate and effective daily activity recognition is an important and fundamental procedure for health condition analysis. One of the most common embedded sensors is 3-axis accelerometer, which can provide useful information for action recognition. Our paper intends to deal with motion recognition problem in a 3-axis accelerometer signal dataset collected by Hong Kong Applied Science and Technology Research Institute Company Limited (ASTRI) using a whist band.

Converting time series recognition problem into image classification problem has been proposed by some literature. [1] presents two encoding methods for one channel series, namely Gramian Angular Field (GAF) and the Markov Transition Field (MTF). Its computation efficiency might be a problem when applied in real-time motion or action recognition. [2] and [3] use recurrence plots (RP) for time series recognition. Though RP can be used to depict the state trajectories, it confuses the tendency of time series which is discovered in our simulation. This problem limits the performance of recognition. They also do not give an encoding solution for 3-dimensional time series like 3-axis accelerometer signals, where correlation information is quite important. Besides, the majority of literatures on activity recognition from 3-axis accelerometers require preprocessing procedures in order to obtain data or features with high quality [4] [5] [6]. Some of them also combine other sensors like gyroscope [7] or camera [8] to enhance accuracies. However, the ASTRI Motion dataset is user-independent and left-right-hand-equivalent. Data are collected from 11 subjects (left, right or both hand) using whist band with sampling rate 52 Hz. No gyroscope is used and the orientation of 3-axis accelerometer is not fixed. These result in large variance and noise in the data of each class and make the recognition challenging.

In this paper, we transform 3-channel accelerometer signals as color images using a modification of RP and train a deep learning model to do classification. RP is originally used in the analysis of dynamic systems and has a shortage in distinguishing tendency when doing time series recognition. We first modify RP to improve our model's performance. Recently, as deep learning has been proven to be successful in image classification tasks [9], we tune a pretrained deep learning model so that it obtains satisfactory results in relative small size datasets. We evaluate our approach by comparing with some state-of-the-arts on both ASTRI Motion dataset and a public dataset named ADL dataset. It shows that our method has achieved highly competitive accuracies.

This work makes the following contributions:

- For the first time, we propose a modified recurrence plot for encoding 3-axis signals into 3-channel color images. Experiments show it can characterize the curve shape in time domain and the correlation among different channel signals as well.
- We propose a simple and effective framework for action recognition, which does not require preprocessing procedures on raw signals and achieves more competitive performance than other state-of-the-art algorithms
- By pretraining step, our deep learning method can be adapted well to small size datasets.

We organize the rest of the paper as follows. Section 2 discusses related work on motion recognition algorithms using a single 3-axis accelerometer sensor. Section 3 introduces a general overview of the proposed recognition framework at first and then describes how a modification of RP is utilized to encode 3-axis signals as color images and how 18-layer ResNet is trained to classify acceleration data traces. In Section 4, we evaluate our system's performance by comparing with other state-of-the-art algorithms by experiments. Detailed analysis of results is also provided. Finally, Section 5 concludes the paper.

2 Related Work

HAR on data from single 3-axis accelerometer has been considerable in the past [10]. In this section, we focus on previous works, which are more representative and relevant to our application. The existing classification methods may be categorized into three groups according to input types.

The first methods rely on heuristic handcrafted features, including statistics (mean, standard deviation, minimum, maximum, covariance), wavelet transform, energy [11] [12] etc. These features are fed into classification models like Support Vector Machine (SVM) [13], Hidden Markov Model (HMM) [14]. The performance of such methods largely depends on the quality of features extracted and requires specific domain knowledge [15] [16]. Moreover, the computational complexity of generative models like HMM is directly proportional to the number of the feature vectors.

The seconds focus on the time domain shape of signal instances themselves instead. Dynamic Time Wrapping (DTW) is one of the most popular and effective methods of this category [17]. DTW has been proven to be a good approach to measure the similarity between two set of time series, possibly of different durations. [18] and [19] are two representative works. [18] provides a combination framework of k -Nearest Neighbor (k -NN) and DTW. This method has been empirically proven to have excellent classification performance and very difficult to beat [20] [21]. [19] employs affinity propagation using DTW to find exemplars for each class and projects all candidates and test samples into lower dimensional space for classification. This method also achieved good performance. The drawback of these two methods is caused by the computation of similarity matrix among large database. When real-time recognition systems are required, they may fall in speed predicament although there are some speed-up DTW algorithms [22] [23]. In addition, deep convolutional neural network can operate on raw time series directly [24] [25]. [25] captures salient patterns of accelerometer signals at different time scales using their defined CNN structure. The problem of self-defined CNN is that large size dataset is required for training. Consequently, it does not perform well in our dataset.

Unlike the former two kinds of methods, the last encode time domain signals as images so as to take full advantage of the powerful distinguish ability of deep learning architectures in computer vision to learn features or patterns [1] [3]. [1] uses polar coordinates to encode time series as two types of images, Gramian Angular Fields (GAF) and Markov Transition Fields (MTF). [3] utilizes recurrence plots to visualize time series. Both of them are only focusing on visualizing the shape of 1D time series and use self-defined CNN framework to do classification. It is also difficult to train well if data is not sufficient.

Inspired by works [2] [3] [26], we provided a method that encodes x-, y- and z-axis of accelerometers to red, green and blue channels of images. To best of our knowledge, our approach is the first to characterize the correlation among x-, y-, z-channel of accelerometers by encoding time signals as different channels of images using a modified RP, so that both of their within-channel and between-channel features can be distinguished by colors. Besides, we tune a deep neural network for classification.

Code is publicly available at <https://github.com/lulujianjie/accelerometer-signal-recognition-using-ResNet-18-and-modified-Recurrence-Plots>

3 Approach

3.1 Overview

The general overview of the proposed action recognition framework is shown as Fig. 1. Notice our framework is simple and no extra preprocessing like average filtering is needed. It can be regarded as two stages. First, we project each channel signal as a square matrix using modified RP respectively and combine them into a color image. After that, we use a fine-tuned 18-layer ResNet to implement classification task.

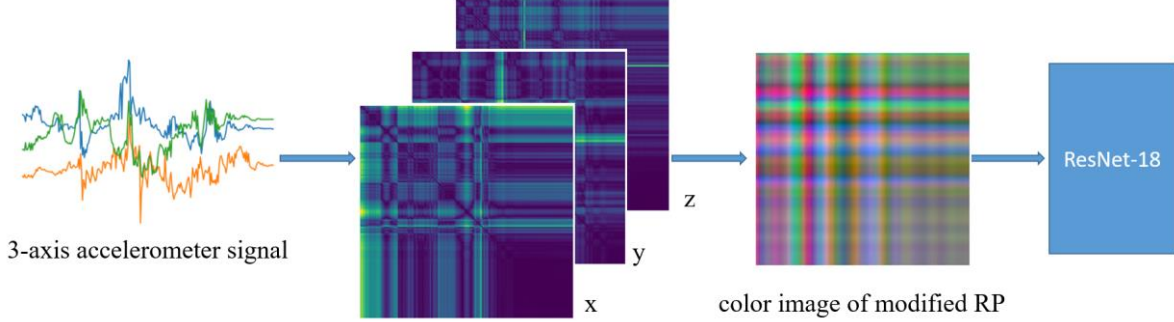


Fig. 1. General overview of proposed action recognition framework¹

3.2 Encoding Accelerometer Signals as Images

Recurrence plot (RP) is originally a visualization tool to study complex dynamic systems. It is first proposed in [27]. [28] and [29] introduce its principles and applications in detail. Recurrence is a concept for analyzing nonlinear data points on phase space trajectories of a dynamical system, whose states are typically in a rather intricate manner. In next sections, we denote vectors by bold lower case letters, e.g., \mathbf{x} , and matrices by bold upper case letters, e.g., \mathbf{R} . The RP can be formally expressed by matrix \mathbf{R} given a trajectory data sample $\mathbf{x} = [x_1, \dots, x_N]$.

$$\mathbf{R}_{i,j}(\varepsilon) = \Theta(\varepsilon - \|\mathbf{x}_i - \mathbf{x}_j\|), \quad i, j = 1, \dots, N \quad (1)$$

where ε is a threshold and determines the number of states, Θ is the unit step function, $\|\cdot\|$ is a norm.

An appropriate norm has to be selected to compute a recurrence matrix. The most common used norms are the L_1 -norm, the L_2 -norm and the L_∞ -norm. Considering a fixed threshold ε , L_∞ -norm is often used since it finds the most amount of neighbors [28]. In our paper, we use L_2 -norm because we skip the threshold step to avoid curve shape loss, which is similar to previous work [3]. Recurrence plot contains typical small-scale features including dots and lines. The large-scale textures can be visually represented by homogenous, periodic, drift and disrupted. Fig. 2 depicts how RP can characterize time series shape features well.

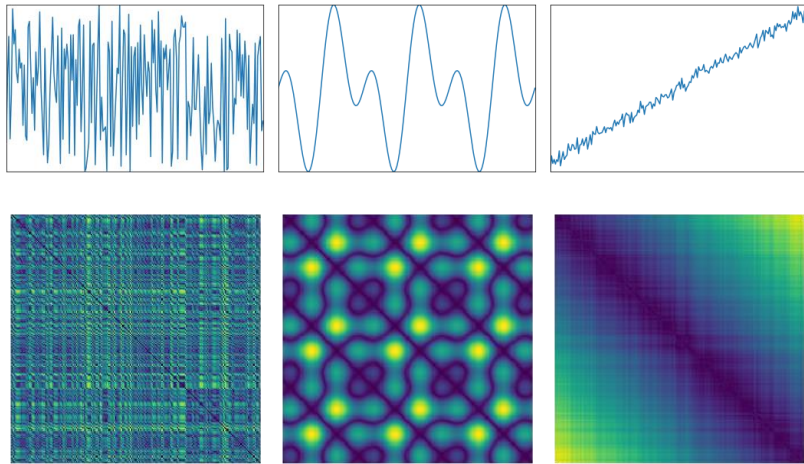


Fig. 2. Recurrence plots of typical signals (top row: time series; bottom row: corresponding recurrence plots; from left to right: white noise, harmonic oscillation with two frequencies and linear drift curve)

We resort RP to encoding 3-axis signals as RGB channels of color images so that their correlation information can be exploited. Mathematically, given a segment of motion data $\mathbf{D}_i = \{\mathbf{x}_i, \mathbf{y}_i, \mathbf{z}_i\}$, where $\mathbf{D}_i \in \mathbb{R}^{3 \times N}$. Each row component in \mathbf{D}_i is a $1 \times N$ vector, whose elements represent the acceleration in the x-, y-, z-direction correspondingly. As our focus is on the formulation method, we take a data sample $\mathbf{x}_i \in \mathbb{R}^d$ as an example and denote x_i^j as j_{th} data point of \mathbf{x}_i . States in phase space can be represented by $\mathbf{s}_i^j: (x_i^j, x_i^{j+1})$, where $\mathbf{s}_i^j \in \mathbb{R}^2$. The RP can be formulated by a recurrence matrix \mathbf{RP} , where $\mathbf{RP} \in \mathbb{R}^{(N-1) \times (N-1)}$, whose elements $\mathbf{RP}_{m,n}$ is the L_2 -norm of a state difference vector.

$$\mathbf{RP}_{m,n} = \|\mathbf{s}_i^m - \mathbf{s}_i^n\| \quad (2)$$

As shown in equation (2), recurrence matrix is symmetric with respect to the zero main diagonal.

However, this symmetry will confuse the tendency of signals. Here we use two pieces of time series $\boldsymbol{\tau}_1$ and $\boldsymbol{\tau}_2$ to illustrate this problem, where $\boldsymbol{\tau}_1 = [t_1, t_2, t_3]$ and $\boldsymbol{\tau}_2 = [t_3, t_2, t_1]$. Without loss of generality, we assume that $\boldsymbol{\tau}_1$ is monotonically increasing and $\boldsymbol{\tau}_2$ is monotonically decreasing, namely $t_1 < t_2 < t_3$. For the other relationships among t_1, t_2 and t_3 , it represents small-scale fluctuations which are not particular critical in time series classification. The RP matrix of $\boldsymbol{\tau}_1$ and $\boldsymbol{\tau}_2$ are computed by

$$\mathbf{RP}_1 = \begin{bmatrix} \|(t_1, t_2) - (t_1, t_2)\| & \|(t_1, t_2) - (t_2, t_3)\| \\ \|(t_2, t_3) - (t_1, t_2)\| & \|(t_1, t_2) - (t_1, t_2)\| \end{bmatrix} \quad (3)$$

and

$$\mathbf{RP}_2 = \begin{bmatrix} \|(t_3, t_2) - (t_3, t_2)\| & \|(t_3, t_2) - (t_2, t_1)\| \\ \|(t_2, t_1) - (t_3, t_2)\| & \|(t_3, t_2) - (t_3, t_2)\| \end{bmatrix} \quad (4)$$

Their recurrence matrixes are same actually, though they are in different tendency obviously. As a consequence, it is difficult to distinguish actions where tendencies play a key role, like sitting, lying and standing. Fig. 3 give a visualization of the tendency confusion problem.

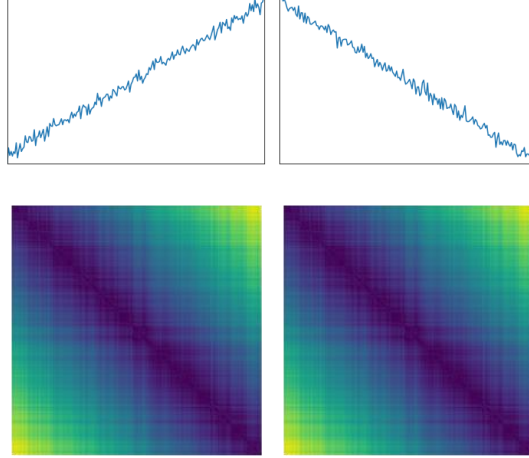


Fig. 3. Tendency confusion problem of recurrence plots (top row: time series; bottom row: corresponding recurrence plots; although they have opposite gradients, their recurrence plots are in the same pattern)

We address this problem by modifying RP. Note that the gradient direction information is vanished due to using norm. For time series whose tendency is uphill, their state difference vector falls in the first quadrant of Cartesian coordinate system while for those in downhill tendency, the state difference vector falls in the third quadrant. So we can use the angle between a baseline vector \mathbf{v} and the state difference vector $\mathbf{s}_i^j - \mathbf{s}_i^{j+1}$ to distinguish different gradient directions. Mathematically, a sign function is used whose formulation is given by,

$$\text{sign}(m,n) = \begin{cases} 1, & \text{if } \frac{(\mathbf{s}_i^m - \mathbf{s}_i^n) \cdot \mathbf{v}}{\|(\mathbf{s}_i^m - \mathbf{s}_i^n)\| \cdot \|\mathbf{v}\|} > \cos\left(\frac{3}{4}\pi\right), \text{ where } \mathbf{v} = [1,1] \\ -1, & \text{otherwise} \end{cases} \quad (5)$$

Hence, the modified RP matrix is constructed by

$$RP_{m,n} = \text{sign}(m,n) \cdot \|s_i^m - s_i^n\| \quad (6)$$

This simple modification of RP improves the performance of our framework considerably. We also show it by implementing experiments in Section 4.

Following the procedures above, we can transform signals $x_i, y_i, z_i \in \mathbb{R}^N$ into three RP matrixes. In order to better depict the correlation among different axis signals, we combine the RP matrixes of x_i, y_i and z_i into a new square matrix M , where $M \in \mathbb{R}^{(N-1) \times (N-1) \times 3}$. Before generating a color image I , normalization needs to be implemented as follows:

$$I_{m,n} = \frac{M_{m,n} - \min_{m,n}(M_{m,n})}{\max_{m,n}(M_{m,n}) - \min_{m,n}(M_{m,n})} \times 255 \quad (7)$$

Finally, accelerometer signals have been encoded as images. Note the diagonals of recurrence matrix are zero. So $\min_{m,n}(M_{m,n})$ should be computed after repelling zero value. Fig. 4 shows that our encoding method can capture the correlation among x-, y-, z- channel signals by colors and their tendencies by its asymmetry as well.

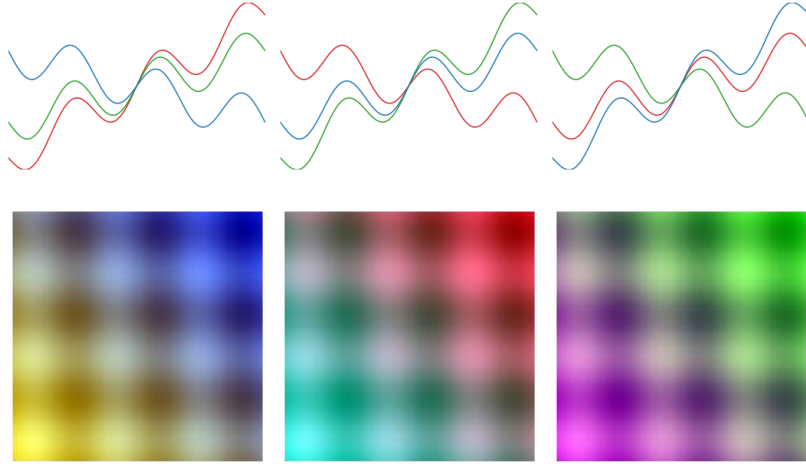


Fig. 4. Different modified RP images of accelerometer signals with various correlation and tendency (top row: raw signals, where red, green and blue represent x-, y-, z- channel of signals; bottom row: corresponding recurrence plots which are asymmetry)

3.2 Classification using residual neural network

We resort to ResNet to do classification of color modified RP images, since it has led some breakthroughs in image classification [30]. ResNet is proposed to solve the problem that deeper models are more difficult to optimize and achieves best accuracies in multiple image recognition tasks. Another reason for using ResNet is that the number of learning parameters tends to be less than other deep learning architectures. It might require relatively small dataset for training. The main element in ResNet is residual block as shown in Fig. 5. Each block has two 3×3 convolutional layers. It copies the learned layers from the shallower model and uses an additional layer for identity mapping.

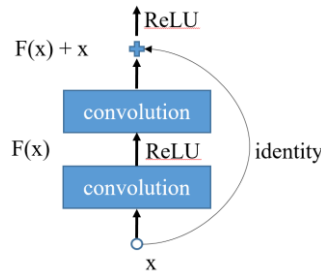


Fig. 5. Residual block

Considering the size of our datasets, we restrict the number of layers to 18. The 18-layer ResNet (ResNet-18) is constructed by stacking residual blocks. We perform downsampling directly by convolutional layers with a stride 2. Batch normalization is applied after each convolutional layer. At the end of the model, a fully-connected layer with softmax is used.

Training ResNet-18 on our dataset with random initialization does not produce accurate recognition results. This is because the size of datasets leads to the model overfitting. To address this, we begin with the model trained on ImageNet [31], and further train or fine-tune the network on our dataset at learning rate 0.001 with a factor of 0.1 every 7 epochs decay. In the training stage, the network is updated for 200 iterations with a batch size of 16. Fig. 6 and Fig. 7 provide some input samples from each label in ASTRI dataset and ADL dataset respectively.

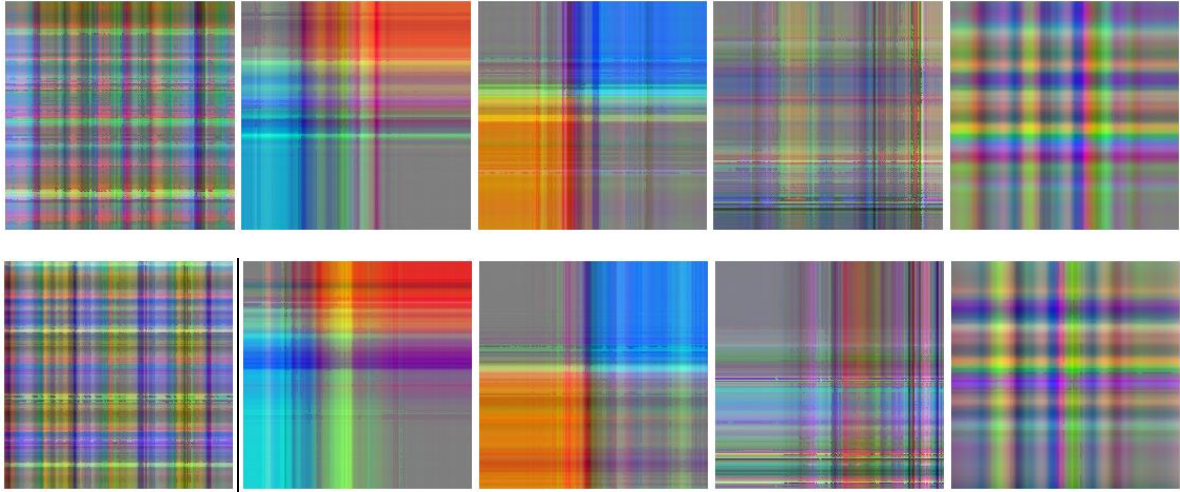


Fig. 6 modified RP images of samples from each label (from left to right: walking, sitting, standing, lying and squatting) in ASTRI Motion dataset

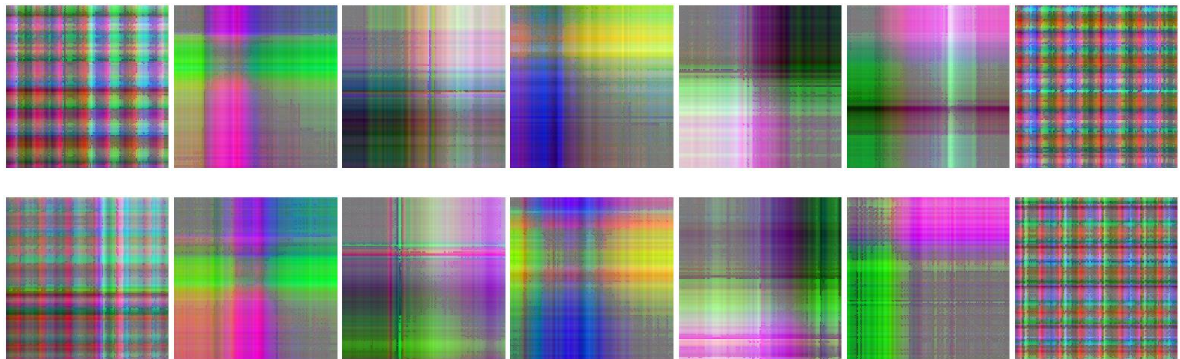


Fig. 7 modified RP images of samples from each label (from left to right: climb stairs, drink water, getup bed, power water, sit down, stand up and walk) in ADL dataset

Each image is generated from a raw 3-axis accelerometer signal sample by applying the modification of RP. The features of data samples from different labels can be depicted by the image patterns including color, textures and their asymmetry attributes show tendencies of the signals. More visualization of these datasets can be found in our open source link.

4 Experiments

4.1 Dataset

We implement experiments on two datasets. The first dataset ASTRI Motion is provided by ASTRI. They collected data using whist band created by themselves. Our framework is originally implemented to address motion recognition in this dataset. To evaluate the generalization ability of our model, we compare the

performance of our model with other state-of-the-art algorithms on a public dataset Activities of Daily Living (ADL) from UCR [32].

ASTRI Motion Dataset This dataset is about five types of human’s hand movements. Data are collected from a single accelerometer configured on the wrist band. In this dataset, 11 subjects wearing smart wrist band conduct activities including walking, sitting, standing, squatting and lying. Each subject performs several times. The wrist band can be worn on either left or right hand and has high sampling rate (52Hz). So these may contribute to the orientation variant and noisy signals. The total number of samples is 1081 including 321 walking, 191 standing, 189 squatting, 193 sitting and 187 lying.

ADL Dataset This dataset records 16 volunteers performing different simple ADL. Data are collected by a single 3-axis accelerometer at sampling rate 32Hz. There are 689 raw data samples used in our experiments. Including 102 climb stairs, 96 drinking water, 101 getup bed, 100 pour water, 96 sit down, 95 stand up and 99 walk.

4.2 Experimental Settings

We compare our approach with the following four baselines, namely 1D-CNN, DTW+ I -NN, AP+DTW and RP+ResNet. Among them, the first three methods show the state-of-the-arts results on recognition of 3-axis accelerometer signals. RP+ResNet are used to evaluate the improvement of our model using modified RP images.

- **1D-CNN** [25] In this baseline, a new architecture of the Convolutional Neural Network (CNN) is used as the classifier. The model operates on batches of raw time series samples directly. ReLU and normalization layers are used in the first four layers, which is same as [25].
- **DTW+ I -NN** [18] Dynamic Time Warping (DTW) is used to compute the distance between training samples and test samples. After getting the distance matrix of accelerometer signals, k -NN is applied to perform classification. Specifically, we select I -NN as the baseline after comparing models with different k values since it obtains the best results.
- **AP+DTW** [19] This approach is proposed on recognition data from a single 3-axis accelerometer and achieves extremely high accuracies. Same as the DTW+ I -NN model, DTW is used as the measurement of distance. Affinity propagation (AP) algorithm is applied for clustering efficiently. After training, the test trace is compared to the exemplars induced by AP and a subset of coordinate traces is selected. All of them are projected onto a subspace for recognition.
- **RP+ResNet** 3-axis accelerometer signals are encoded as images using original RP. Image classification task is also implemented based on ResNet-18. We use this model to compare and evaluate whether our method has tackled the tendency confusion problem.

For better application in practice, we do not distinguish the left or right hand, age and gender of subjects. A 5-second window is applied in our experiments since this time duration should be sufficient for subjects to finish actions, such as sitting and lying. The dataset distribution with respect to class labels has described in Section 4.1. We split dataset as training set and testing set according to 7:3. All experiments are implemented following this percentage without preprocessing like average filtering.

4.3 Experimental Results

Experimental results of our methods and the other four baseline methods on ASTRI Motion dataset and ADL dataset are shown in Table 1 and Table 2 respectively. The best performance for each class is highlighted in bold.

Table 1 Comparison of Performance of Proposed method and other baselines on ASTRI Motion Dataset

	Accuracy (%)					
	Walking	Sitting	Standing	Squatting	Lying	Average
1D-CNN	85.22	87.75	81.25	77.55	71.43	81.24
DTW+1-NN	53.33	84.48	93.44	91.80	57.40	73.41
DTW+AP	1.310	94.22	82.10	82.63	46.30	54.93
RP + ResNet-18	90.97	96.83	79.27	81.15	79.14	86.19
Proposed Method	93.77	82.90	89.01	95.77	87.17	90.20

Table 2 Comparison of Performance of Proposed method and other baselines on ADL Dataset

	Accuracy (%)							Average
	Climb stairs	Drink glass	Getup bed	Pour water	Sit down	Stand up	Walk	
1D-CNN	76.47	83.33	67.33	83.00	51.04	76.84	70.71	72.71
DTW-1NN	77.14	94.27	65.71	92.86	89.72	93.67	71.26	83.32
DTW+AP	59.05	93.75	65.31	90.59	97.29	68.35	88.51	80.22
RP + ResNet-18	79.17	83.33	64.71	83.56	84.38	78.46	81.53	79.26
Proposed Method	83.33	96.88	81.19	94.00	93.75	91.59	85.86	89.41

From the experimental results, our method obtains best average performance than the others in both datasets.

In comparison, 1D-CNN achieves plain results in both datasets, though its training accuracy achieves 100%. This is mainly caused by small dataset size. In [25], CNN shows good feature extraction capabilities. But the model is trained in a dataset with 136869 samples, which is far more than our datasets. It also shows the overfitting problem that the recognition performance on ASTRI Motion dataset with 1081 samples is slightly better than that on ADL with 689 samples. In addition, our dataset is subject-independent, which is different from the experiments in [25].

DTW-1NN performs the best accuracy on some actions like standing. It achieves second highest average accuracy in ADL dataset. But it does not obtain satisfactory results in other actions, for example walking in ASTRI Motion dataset. The possible reason may lie in the large variance within class, which is caused by mixing subjects. They differ from one person to another and even the same subject cannot perfectly replicate the same action. For some samples from different actions, they even have similar patterns in time domain. As a result, DTW does not work effectively.

The same problem occurs in DTW+AP since it also depends on DTW heavily. Another problem may be from the clustering algorithm AP. AP does not guarantee that all members of a cluster have the same label as their exemplar. Moreover, the exemplars tend to have unbalanced distribution in terms of labels, which is observed in our experiments. For instance, 166 exemplars are learned while there are only 16 exemplars from walking samples.

After modifying RP, it improves the recognition performances considerably by comparing proposed method with RP+ResNet-18. Although same ResNets are implemented for classification, our method achieves better accuracies in four of five classes of ASTRI Motion dataset and all classes of ADL dataset than RP+ResNet-18.

We also consider the efficiency of our method. All experiments are conducted on a PC, which has an Intel i5-7500, 8G RAM and a GTX1060 6G GPU. The training time of our model is around 20 minutes. For recognition stage, 4 raw instances are first encoded as images and predicted with in a second. Note that each instance is 5-second data. Thus our framework is competent in real-time recognition task.

Experimental results show that the modification of RP proposed in this paper has good capacity to characterize the curve shape of accelerometer signals and the correlation among different axes. Resorting to the powerful distinguish ability of ResNet in image classification, we obtain satisfactory results in both small size datasets. Its efficiency is good enough for real-time application.

5 Conclusions

In conclusion, we propose an efficient and effective activity recognition framework based on data from a single 3-axis accelerometer. Our framework encodes accelerometer signals as color images using recurrence plots (RP). Modified RP is first proposed to solve its tendency confusion problem. After obtaining images of time series signals, we tune an 18-layer ResNet that is pretrained in ImageNet to implement classification. Finally, we test and evaluate our method on two datasets. Experimental results have shown that our framework achieves highly competitive recognition accuracies when compared to the other state-of-the-art methods in the literature. It shows good potential for 3-axis accelerometer signals recognition in small size datasets.

Acknowledgement

Authors really appreciate Hong Kong Applied Science and Technology Research Institute Company Limited (ASTRI) for providing data for this research.

References

- [1] Wang, Z., & Oates, T. Encoding time series as images for visual inspection and classification using tiled convolutional neural networks. In Workshops at the Twenty-Ninth AAAI Conference on Artificial Intelligence (pp. 40-46).
- [2] Silva, D. F., De Souza, V. M., & Batista, G. E. Time series classification using compression distance of recurrence plots. In Data Mining (ICDM), 2013 IEEE 13th International Conference on (pp. 687-696). IEEE.
- [3] N Hatami, Y Gavet, J Debayle. Classification of Time Series Image using Deep CNN. arXiv preprint arXiv:1710.00886
- [4] Casale, P., Pujol, O., & Radeva, P. Human activity recognition from accelerometer data using a wearable device. In Iberian Conference on Pattern Recognition and Image Analysis (pp. 289-296). Springer, Berlin, Heidelberg.
- [5] Mathie, M. J., Celler, B. G., Lovell, N. H., & Coster, A. C. F. Classification of basic daily movements using a triaxial accelerometer. *Medical and Biological Engineering and Computing*, 42(5), 679-687.
- [6] Khan, A. M., Lee, Y. K., Lee, S. Y., & Kim, T. S. A triaxial accelerometer-based physical-activity recognition via augmented-signal features and a hierarchical recognizer. *IEEE transactions on information technology in biomedicine*, 14(5), 1166-1172.
- [7] A. Yang, S. Iyengar, S. Sastry, R. Bajcsy, P. Kuryloski, and R. Jafari, "Distributed segmentation and classification of human actions using a wearable motion sensor network," in Proc. IEEE Comput. Soc. Conf. Comput. Vision and Pattern Recogn. Workshops (CVPRW '08), Jun. 2008, pp. 1–8
- [8] Zou, Q., Ni, L., Wang, Q., Li, Q., & Wang, S. Robust gait recognition by integrating inertial and RGBD sensors. *IEEE transactions on cybernetics*.
- [9] LeCun, Y., Bengio, Y., & Hinton, G. Deep learning. *nature*, 521(7553), 436.
- [10] Lara, O. D., & Labrador, M. A. A survey on human activity recognition using wearable sensors. *IEEE Communications Surveys and Tutorials*, 15(3), 1192-1209.
- [11] Bulling, A., Blanke, U., & Schiele, B. A tutorial on human activity recognition using body-worn inertial sensors. *ACM Computing Surveys (CSUR)*, 46(3), 33.
- [12] Rezvanian, S., & Lockhart, T. E. Towards real-time detection of freezing of gait using wavelet transform on wireless accelerometer data. *Sensors*, 16(4), 475.
- [13] Xing, Z., Pei, J., & Keogh, E. A brief survey on sequence classification. *ACM Sigkdd Explorations Newsletter*, 12(1), 40-48.
- [14] Mannini, A., & Sabatini, A. M. Accelerometry-based classification of human activities using Markov modeling. *Computational intelligence and neuroscience*, 2011, 4.
- [15] Plötz, T., Hammerla, N. Y., & Olivier, P. Feature learning for activity recognition in ubiquitous computing. In *IJCAI Proceedings-International Joint Conference on Artificial Intelligence (Vol. 22, No. 1, p. 1729)*.
- [16] Huynh, T., & Schiele, B. Analyzing features for activity recognition. In *Proceedings of the 2005 joint conference on Smart objects and ambient intelligence: innovative context-aware services: usages and technologies*(pp. 159-163). ACM.
- [17] Rakthanmanon, T., Campana, B., Mueen, A., Batista, G., Westover, B., Zhu, Q., Zakaria, J., Keogh, E.: Searching and mining trillions of time series subsequences under dynamic time warping. In: *Proceedings of the*

18th ACM SIGKDD International Conference on Knowledge Discovery and Data Mining, KDD 2012, p. 262 (2012)

[18] Zhang, Y., & Glass, J. R. An inner-product lower-bound estimate for dynamic time warping. In Acoustics, Speech and Signal Processing (ICASSP), 2011 IEEE International Conference on (pp. 5660-5663). IEEE.

[19] Akl, A., Feng, C., & Valaee, S. A novel accelerometer-based gesture recognition system. IEEE Transactions on Signal Processing, 59(12), 6197-6205.

[20] Ding, H., Trajcevski, G., Scheuermann, P., Wang, X., & Keogh, E. Querying and mining of time series data: experimental comparison of representations and distance measures. Proceedings of the VLDB Endowment, 1(2), 1542-1552.

[21] Batista, G.E.A.P.A., Wang, X., Keogh, E.J.: A complexity-invariant distance measure for time series. In: SIAM Conf. Data Mining (2011)

[22] X. Xi, E. Keogh, C. Shelton, L. Wei, and C. A. Ratanamahatana, "Fast time series classification using numerosity reduction," Proc. ICML'06, pp. 1033–1040, 2006

[23] Sakurai, Y., Yoshikawa, M., & Faloutsos, C. FTW: fast similarity search under the time warping distance. In Proceedings of the twenty-fourth ACM SIGMOD-SIGACT-SIGART symposium on Principles of database systems (pp. 326-337). ACM.

[24] Kiranyaz, S., Ince, T., & Gabbouj, M. Real-time patient-specific ECG classification by 1-D convolutional neural networks. IEEE Transactions on Biomedical Engineering, 63(3), 664-675.

[25] Yang, J., Nguyen, M. N., San, P. P., Li, X., & Krishnaswamy, S. Deep Convolutional Neural Networks on Multichannel Time Series for Human Activity Recognition. In IJCAI (pp. 3995-4001).

[26] Souza, V. Silva, D. Batista, G. Extracting Texture Features for Time Series Classification, 1425-1430, International Conference on Pattern Recognition (ICPR), 2014.

[27] Eckmann, J. P., Kamphorst, S. O., & Ruelle, D. Recurrence plots of dynamical systems. EPL (Europhysics Letters), 4(9), 973.

[28] Marwan, N., Romano, M. C., Thiel, M., & Kurths, J. Recurrence plots for the analysis of complex systems. Physics reports, 438(5-6), 237-329.

[29] Marwan, N. A historical review of recurrence plots. The European Physical Journal Special Topics, 164(1), 3-12.

[30] He, K., Zhang, X., Ren, S., & Sun, J. Deep residual learning for image recognition. In Proceedings of the IEEE conference on computer vision and pattern recognition (pp. 770-778).

[31] Russakovsky, O., Deng, J., Su, H., Krause, J., Satheesh, S., Ma, S., ... & Berg, A. C. Imagenet large scale visual recognition challenge. International Journal of Computer Vision, 115(3), 211-252.

[32] Bruno, B., Mastrogiovanni, F., & Sgorbissa, A. A public domain dataset for ADL recognition using wrist-placed accelerometers. In Robot and Human Interactive Communication, 2014 RO-MAN: The 23rd IEEE International Symposium on (pp. 738-743). IEEE.